

1 Sorption of lead by Salisbury biochar produced from British broadleaf hardwood

2
3 Zhengtao Shen ^{a,*}, Fei Jin ^a, Fei Wang ^a, Oliver McMillan ^a, Abir Al-Tabbaa ^a

4
5
6 ^a(Geotechnical and Environmental Research Group, Department of Engineering,
7
8 University of Cambridge, Cambridge, CB2 1PZ, United Kingdom)
9

10
11 * Corresponding author: Email: ztshennju@gmail.com; zs281@cam.ac.uk. Phone
12
13 number: 0044+7541935253. Fax: 0044+7541935253
14

15
16 Abstract: In this study, the physicochemical properties of Salisbury biochar
17
18 produced from British broadleaf hardwood and its adsorption characteristics
19
20 towards lead was investigated. The biochar particle size has a significant effect
21
22 on its BET surface area, cation exchange capacity and sorption of lead. The
23
24 kinetics data were well fitted by the Pseudo second order model. The increase
25
26 of biochar dosage increased the percentage of lead removal in solutions. The
27
28 increase of initial solution pH increased the percentage of lead removal across
29
30 the pH range of 2 - 10. The calculated maximum adsorption capacity of lead by
31
32 Langmuir model were 47.66 and 30.04 mg/g for 0.15 mm and 2 mm samples.
33
34 The adsorption capacities of different metals decreased in the order of lead >
35
36 nickel > copper > zinc calculated in mmol/g. This study suggests a great
37
38 potential of biochars derived from British broadleaf hardwood to be applied in
39
40 soil remediation.
41
42
43
44
45

46
47 Keywords: Adsorption, Lead, Salisbury biochar, British hardwood, Heavy metals
48
49
50
51
52
53
54
55
56
57
58
59
60
61
62
63
64
65

1 1. Introduction
2

3 Biochar, as a carbon storage material, is produced by heating biological
4 residues with the exclusion of air (Sohi, 2012). Recently, the potential
5 application of biochar in soil remediation has been investigated. When applied
6 in contaminated soils, the benefits of biochar are: 1) the high sorption capacity
7 helps to immobilise the heavy metals and organic pollutants (Beesley et al.,
8 2011) 2) the enhancement of fertility and resilience of soil by biochar addition
9 can help the greening and restoration of the contaminated land (Sohi, 2012) 3)
10 the sequestration of CO₂ by storing carbon in a more recalcitrant form (Sohi,
11 2012).
12
13
14
15
16
17
18
19
20
21
22
23
24

25 Before undertaking field trials, it is necessary to identify a feedstock that is
26 readily available and renewable, and to investigate its performance in removing
27 contaminants from soil and water. Biochar from hardwood is able to treat both
28 organic and inorganic contaminants according to the principles proposed by
29 Beesley et al. (2011). In a previous study, Salisbury biochar, which is made
30 from British broadleaf hardwood, was applied to an industrial contaminated site
31 in Yorkshire, UK in 2011 (Shen et al., 2015). The three-year study that followed
32 observed a good performance for Salisbury biochar in immobilising heavy
33 metals in soils (Shen et al., 2015). Likewise, Gomez-Eyles et al. (2011) applied
34 Salisbury biochar to calcareous contaminated-soil and observed that the
35 treatment successfully reduced the bioavailability of organic contaminants as
36 well as the concentration of water soluble Cu²⁺. In the UK, 31% of the total
37 productive woodland, which covers 10.6% of the entire land area, is
38 broadleaved (Thurkettle, 1997). According to a recent forecast, the average
39
40
41
42
43
44
45
46
47
48
49
50
51
52
53
54
55
56
57
58
59
60
61
62
63
64
65

1 annual hardwood availability for the UK forest estate is at least 1.6 million m³
2
3 over the next 50 years and may be up to 6.25 million m³ (National Forest
4
5 Inventory, UK, 2014).
6

7
8 Based on this evidence, British hardwood is potentially a suitable feedstock
9
10 both in terms of its high efficiency in removing contaminants from soil and its
11
12 reliable future availability. However a systematic adsorption characterisation for
13
14 this kind of biochar has not been carried out yet; this is important for
15
16 understanding the sorption mechanisms involved and will aid the design of
17
18 future field-scale remediation projects.
19
20

21
22 This study focused on the adsorption characterisation for heavy metals to
23
24 Salisbury biochar. Lead was selected for the sorption studies as it is among the
25
26 most serious concerns for water and soil pollution (Yang et al., 2014). The
27
28 kinetics, the influence of biochar dosage, particle size and the pH of the solution
29
30 on adsorption of lead on biochar, the adsorption isotherms and the comparison
31
32 of the adsorption capacity of lead with those of copper, nickel and zinc were
33
34 investigated. The aims of this study were to highlight the potential application of
35
36 Salisbury biochar in soil remediation and to give validation for its future practical
37
38 application.
39
40
41
42
43
44

45 2 Materials and methods

46 2.1 Physicochemical properties of biochar

47
48 Salisbury biochar was obtained from Southern Woodland products (Salisbury,
49
50 UK). It was produced from British broadleaf hardwood at a pyrolysis
51
52 temperature of 600 °C. The biochar was dried at 40 °C for 48 h in an oven and
53
54 sieved to smaller than 0.15 mm and 2 mm respectively for further analysis.
55
56
57
58
59
60
61
62
63
64
65

1 Throughout this paper, the terms “0.15 mm” and “2 mm” will be used to
2 represent the biochar samples sieved to smaller than 0.15 mm and 2 mm
3 respectively.
4
5
6

7
8 The BET surface area, cation exchange capacity (CEC), pH, carbon and
9 nitrogen contents and the total contents of trace elements of biochar were
10 determined. The infrared spectrum of biochar was tested by Fourier transform
11 infrared spectroscopy (FTIR) spectrometer. The surface morphology of biochar
12 was examined by scanning electron microscopy (SEM). The details of these
13 test methods are presented in Appendix A.
14
15
16
17
18
19
20
21

22 2.2 Sorption studies

23
24 The kinetics of Pb^{2+} adsorption, the influence of biochar dosage and solution pH
25 on Pb^{2+} adsorption and the isotherms of Pb^{2+} , Cu^{2+} , Ni^{2+} and Zn^{2+} adsorption
26 onto biochar were studied by laboratory batch tests. The details of these test
27 methods are presented in Appendix A.
28
29
30
31
32
33
34

35 2.3 Statistical analysis

36
37 All the experiments in this study were carried out in duplicates. The means and
38 standard deviations were calculated and presented for each experiment. The
39 significance of the influence of the particle size on BET surface area, CEC and
40 pH of biochar and the influence of biochar dosage, solution pH and particle size
41 on Pb^{2+} adsorption were evaluated by a one-way analysis of variance (ANOVA)
42 at the significance level of 0.05 using SPSS 16.0. Regression was used to
43 evaluate the models predicting the kinetics and equilibrium using Origin 8.5. R
44 square were used to indicate the fitness of the models.
45
46
47
48
49
50
51
52
53
54
55
56

57 3 Results and discussion

3.1 Physicochemical properties of biochar

The physicochemical properties of biochar are shown in Table B.1. The BET surface area and CEC were 54% and 22% lower respectively for the 2 mm biochar (2.46 m²/g and 5.62 cmol/kg) compared with the 0.15 mm biochar (5.30 m²/g and 7.20 cmol/kg), indicating that particle size significantly ($P < 0.001$ for BET surface area and $P < 0.05$ for CEC) influenced the physicochemical properties of the biochar. Whereas the influence of particle size on the pH of biochar was not significant ($P > 0.05$). The pH of biochar in water was slightly lower than 7. The slightly acidic pH values (6.96 and 6.78) of Salisbury biochar in this study may indicate that this biochar retained relatively more carboxyl and acidic groups (Ronsse et al., 2013). The CN analysis revealed that Salisbury biochar mainly contained carbon (79.97%). Elemental analysis showed that the biochar contained less than 0.01% of nickel, copper, zinc and lead, therefore it was assumed that this small part of metals would not affect the sorption studies. The FTIR spectra of Salisbury biochar is shown in Fig. B.1. The biochar has a C-C stretching peak at 1578 cm⁻¹ wavenumbers and a C-H/O-H bending peak at 1428 cm⁻¹ due to the cellulose and hemicellulose in the raw material as well as C-H out-of-plane bending peaks at 1172 and 745 cm⁻¹ wavenumbers due to either lignin or cellulose/hemicellulose in the raw material. SEM images of Salisbury biochar are shown in Fig. B.2 and indicate a porous surface structure on the biochar.

3.2 Adsorption studies

3.2.1 Kinetics

1 The influence of contact time on the adsorbed amount of Pb^{2+} on biochar is
2 shown in Fig. 1. Approximately 66% and 73% of the sorption occurred in the
3 first 3 hours for the 0.15 mm and 2 mm samples respectively. The adsorption
4 rates subsequently reduced as the equilibrium concentrations were approached.
5
6
7
8
9
10
11
12
13
14 (Fig. 1).

15
16 In order to investigate the adsorption mechanism, a pseudo first order model
17 and a pseudo second order model (Table B.2) were used to describe the
18 kinetics of Pb^{2+} adsorption onto biochar. The regression coefficients (R square)
19 using pseudo first order model were low (0.70 and 0.60) (Table B.3) and the
20 fitted model observed a poor fit with the experimental data. The pseudo second
21 order equation fitted the kinetics data well and the regression coefficient was
22 greater than 0.99 (Table B.3). The calculated q_e matched the experimental
23 value well, indicating the Pb^{2+} adsorption on Salisbury biochar follows the
24 pseudo second order model which assumes chemisorption. The Weber and
25 Moris model was used to describe the intraparticle diffusion mechanism. In this
26 study, a linear relationship was observed for both 0.15 mm and 2 mm biochar
27 within the first 3 hours but the trends did not pass through the origin (Fig. B.3),
28 indicating that the intraparticle diffusion is not the rate limiting step during this
29 period.
30
31
32
33
34
35
36
37
38
39
40
41
42
43
44
45
46
47
48

49 3.2.2 The influence of biochar dosages

50
51
52 The percentages of Pb^{2+} removal increased significantly from 72.84% to 98.56%
53 (P < 0.05) for 0.15 mm samples and from 42.57% to 89.61% (P < 0.001) for 2
54 mm samples with the increase of the biochar dosage from 5 to 15 g/L and
55
56
57
58
59
60
61
62
63
64
65

1 remained almost constant beyond 25 g/L (Fig. 2a). The amount of Pb^{2+}
2
3 adsorbed per unit adsorbent mass at equilibrium decreased across the biochar
4 dosage range of 5 - 100 g/L (Fig. 2a). This trend may be caused by the
5
6 aggregation between biochar particles and subsequently the unsaturation of
7
8 adsorption sites on biochar surface at high solid concentrations during the
9
10 experiment (Meng et al., 2014).
11
12
13
14

15 3.2.3 The influence of initial solution pH

16
17 The adsorbed Pb^{2+} at initial pH of 2 was the lowest among the pH values tested
18 (26.50% and 21.77% removal degrees for the 0.15 m and 2 mm samples
19 respectively) (Fig. 2b). The increase of solution pH can enhance the
20
21 deprotonation process on biochar surface and create more negative sites that
22
23 enhance the adsorption of Pb^{2+} (Mohan et al., 2014). Hence the amount of Pb^{2+}
24
25 adsorbed was significantly greater at higher initial pH values (99.92% and 92.83%
26
27 removal degrees for the 0.15 mm and 2 mm samples respectively at initial pH of
28
29 10, $P < 0.001$ compared with removal degrees at pH of 2 for both samples) (Fig.
30
31 2b).
32
33
34
35
36
37
38
39

40 Yang et al. (2014) and Kołodyńska et al. (2012) each observed a decrease in
41
42 Pb^{2+} sorption to biochar when the initial pH was greater than 5. In the study of
43
44 Kołodyńska et al. (2012), the equilibrium pH values were higher than 8 when
45
46 the initial pH value was 5 or higher due to the alkalinity of the biochar while
47
48 Yang et al. (2014) did not report the pH of the biochar or the equilibrium pH
49
50 values of the solutions. It was suggested that this decrease in sorption was a
51
52 result of lead precipitation or the formation of lead complex ions at high pH
53
54 values. In this study, a decrease of adsorption capacity of Pb^{2+} onto biochar
55
56
57
58
59
60
61
62
63
64
65

1 was not observed up to an initial pH value of 10 (Fig. 2b). This is most likely due
2
3 to the equilibrium pH values of the solution staying below 7.17 due to the acidity
4
5 of the biochar (Fig. 2b). Precipitation of Pb^{2+} to $Pb(OH)_2$ occurs at a pH of
6
7 approximately 7.70 and was therefore unlikely to be present in significant
8
9 quantities. The finding that the amount of Pb^{2+} adsorbed is greater at higher pH
10
11 values is in line with Mohan et al. (2014) who ensured that precipitation did not
12
13 occur by maintaining the initial and equilibrium solution pH at less than 7.70.
14
15
16
17

18 3.2.4 Adsorption equilibrium

19
20 Pb^{2+} batch adsorption studies were conducted and experimental data were
21
22 fitted by the Langmuir and Freundlich isotherm models. The linear forms of the
23
24 two models (Table B.2) were used in this study because linear forms, rather
25
26 than nonlinear forms, of adsorption isotherms had been applied in over 95% of
27
28 the liquid-phase adsorption systems (Foo and Hameed, 2010). The results are
29
30 shown in Fig. B.4 and Table B.4. The experimental data was well fitted by the
31
32 Langmuir model with an R^2 value of 0.988 for 0.15 mm samples and 0.978 for 2
33
34 mm samples (Table B.4). The equilibrium parameter R_L was used to express
35
36 the essential characteristics of a Langmuir isotherm (Hameed and Ahmad,
37
38 2009). The R_L values in this case were 0.017 for 0.15 mm biochar and 0.049 for
39
40 2 mm biochar, confirming that adsorption of Pb^{2+} to Salisbury biochar is
41
42 favourable under conditions of this study.
43
44
45
46
47
48

49 The Freundlich model was also applied which assumes multilayer adsorption to
50
51 a heterogeneous adsorbent surface (Foo and Hameed, 2010). The Freundlich
52
53 model fit the experimental data closely with R^2 values greater than 0.98 for both
54
55 0.15 and 2 mm samples; the regression constants are given in Table B.4. The
56
57
58
59
60
61
62
63
64
65

1 1/n values were 0.742 and 0.713 for the 0.15 mm and 2 mm samples
2
3 respectively indicating some degree of heterogeneity in the Salisbury Biochar.
4

5
6 The calculated adsorption capacity for Pb^{2+} is compared with that of biochars in
7
8 other studies in Table B.5. Although the BET surface area of this biochar
9
10 (section 3.1) was lower than sugarcane bagasse biochar (14.1 m^2/g), its
11
12 adsorption capacity of lead was much higher, indicating that physical adsorption
13
14 did not dominate the sorption of lead on biochar. Cation exchange or surface
15
16 complexation may have dominated the sorption process as Salisbury biochar
17
18 has a higher CEC capacity and probably more carboxyl groups (which was
19
20 suggested by the lower pH) that favours the formation of complexation with lead
21
22 (Cao et al., 2009). Although some manure-derived biochars reveal a higher
23
24 adsorption capacity than this biochar (Table B.5), their availability was much
25
26 lower compared with the large annual production of hardwood (National Forest
27
28 Inventory, UK, 2014). Therefore, hardwood biochar is a good choice in field-
29
30 scale remediation projects in the UK for its considerable adsorption capacity
31
32 and reliable future availability.
33
34
35
36
37
38
39

40 3.2.5 Influence of particle size

41
42 0.15 mm biochar adsorbed more Pb^{2+} than 2 mm biochar at all times during the
43
44 kinetics study (Fig. 1). 0.15 mm biochar exhibited significantly ($P < 0.001$)
45
46 higher sorption capacity than 2 mm biochar at biochar dosage of 5 g/L (Fig. 2a).
47
48 At initial biochar dosages greater than 25 g/L, the percentages of lead removal
49
50 were very close to 100% for both samples (Fig. 2a). Sorption of Pb^{2+} was higher
51
52 for 0.15 mm biochar than 2 mm biochar across all pH values tested (Fig. 2b).
53
54
55
56
57 The samples with smaller particle size exhibited a higher adsorption capacity
58
59
60
61
62
63
64
65

1 (Table B.4). The better performance of 0.15 mm biochar at Pb^{2+} sorption is
2
3 attributed to both the significantly higher surface area which creates more active
4
5 sites for the sorption of Pb^{2+} and the significantly higher CEC which gives better
6
7 capacity to exchange the metals (Table B.1).
8
9

10 3.2.6 Adsorption capacity of copper, nickel and zinc

11 The adsorption capacity of Cu^{2+} , Ni^{2+} and Zn^{2+} on Salisbury biochar were also
12
13 investigated in order to form a basis for comparison with Pb^{2+} . The experimental
14
15 data were fitted to the Langmuir and Freundlich isotherm models using the
16
17 same methodology as described for Pb^{2+} and the results are shown in Fig. B.5
18
19 and Table B.6. The calculated adsorption capacity by Langmuire model for Pb^{2+} ,
20
21 Cu^{2+} , Ni^{2+} , Zn^{2+} were 0.230, 0.101, 0.105 and 0.098 mmol/g respectively for
22
23 0.15 mm samples (Table B.6), equal to 47.66, 6.42, 6.16 and 6.41 mg/g
24
25 respectively. The higher adsorption capacity of Pb^{2+} by this biochar may be due
26
27 to the stronger surface electrostatic attraction, since the electronegativity
28
29 constant of Pb^{2+} is high (2.33) and plays a significant role in its adsorption
30
31 (Caporale and Pigna, 2014). The formation of surface complexation between
32
33 biochar's carboxyle groups and lead can also contribute to its higher adsorption
34
35 capacity. The release of negatively charged ions such as CO_3^{2-} and PO_4^{3-} may
36
37 also favour the precipitation of lead on the biochar's surface (Cao et al., 2009;
38
39 Liu and Zhang, 2009) which would incerase apparent sorption of Pb^{2+} . However,
40
41 the manure-derived biochars in Kołodyńska et al. (2012) may also contain a
42
43 considerable amount of CO_3^{2-} and PO_4^{3-} . As Kołodyńska et al. (2012) did not
44
45 present the P contents in the biochars, it is hard to make a comparison.
46
47
48
49
50
51
52
53
54
55
56

57 4 Conclusions

58
59
60
61
62
63
64
65

1 It was found that biochar particle size, dosage and the solution pH significantly
2 affect the sorption of lead on biochar. The kinetics data were well fitted by the
3 pseudo second order model. The Salisbury biochar in this study exhibited high
4 adsorption capacity of lead in aqueous solutions compared with both other
5 studies on lead sorption on biochar and other metals in this study. Therefore,
6 given the abundant and renewable source of its feedstock in the UK, biochar
7 derived from British broadleaf hardwood has the potential to be produced on a
8 large scale and applied in soil remediation.
9

10 11 12 13 14 15 16 17 18 19 20 21 22 23 24 25 26 27 28 29 30 31 32 33 34 35 36 37 38 39 40 41 42 43 44 45 46 47 48 49 50 51 52 53 54 55 56 57 58 59 60 61 62 63 64 65

- 20
21
22
23
24
25
26
27
28
29
30
31
32
33
34
35
36
37
38
39
40
41
42
43
44
45
46
47
48
49
50
51
52
53
54
55
56
57
58
59
60
61
62
63
64
65
- References
- Beesley, L., Moreno-Jiménez, E., Gomez-Eyles, J.L., Harris, E., Robinson, B.,
Sizmur, T., 2011. A review of biochars' potential role in the remediation,
revegetation and restoration of contaminated soils. *Environ. Pollut.* 159,
3269–82. doi:10.1016/j.envpol.2011.07.023
- Cao, X., Ma, L., Gao, B., Harris, W., 2009. Dairy-manure derived biochar
effectively sorbs lead and atrazine. *Environ. Sci. Technol.* 43, 3285–3291.
doi:10.1021/es803092k
- Caporale, A.G., Pigna, M., 2014. Effect of pruning-derived biochar on heavy
metals removal and water dynamics 1211–1222. doi:10.1007/s00374-014-
0960-5
- Foo, K.Y., Hameed, B.H., 2010. Insights into the modeling of adsorption
isotherm systems. *Chem. Eng. J.* 156, 2–10. doi:10.1016/j.cej.2009.09.013
- Gomez-Eyles, J.L., Sizmur, T., Collins, C.D., Hodson, M.E., 2011. Effects of
biochar and the earthworm *Eisenia fetida* on the bioavailability of polycyclic

1 aromatic hydrocarbons and potentially toxic elements. Environ. Pollut. 159,
2
3 616–22. doi:10.1016/j.envpol.2010.09.037
4

5
6 Hameed, B.H., Ahmad, a. a., 2009. Batch adsorption of methylene blue from
7
8 aqueous solution by garlic peel, an agricultural waste biomass. J. Hazard.
9
10 Mater. 164, 870–875. doi:10.1016/j.jhazmat.2008.08.084
11

12
13 Inventory, N.F., Commission, F., Ditchburn, B., Brewer, A., 2016. 50-year
14
15 forecast of hardwood timber availability.
16

17
18 Kołodyńska, D., Wnętrzak, R., Leahy, J.J., Hayes, M.H.B., Kwapiński, W.,
19
20 Hubicki, Z., 2012. Kinetic and adsorptive characterization of biochar in
21
22 metal ions removal. Chem. Eng. J. 197, 295–305.
23
24 doi:10.1016/j.cej.2012.05.025
25

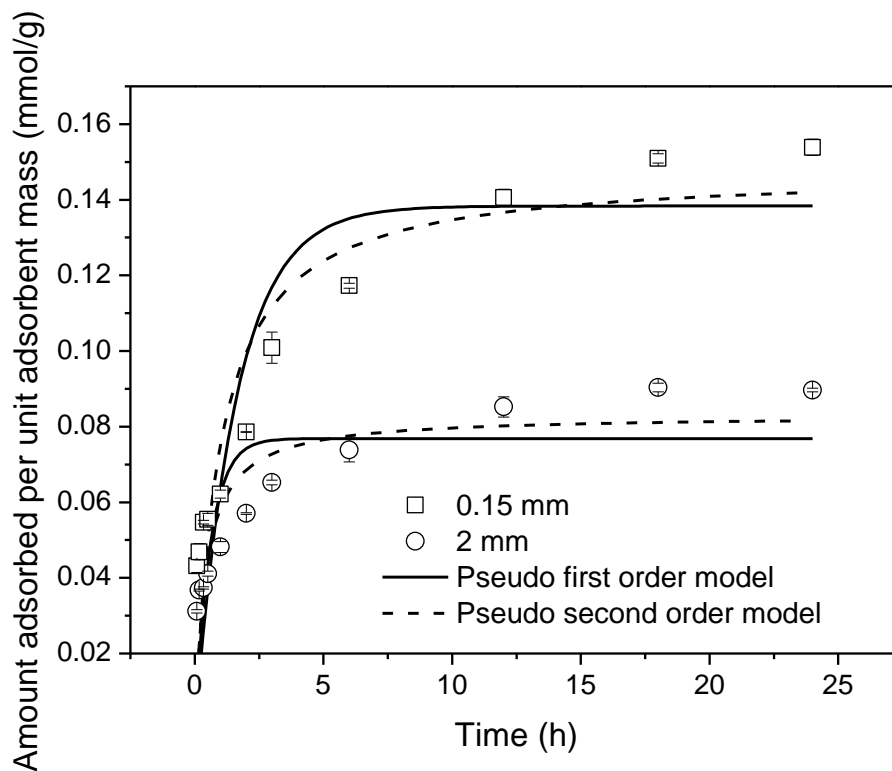
26
27 Liu, Z., Zhang, F.S., 2009. Removal of lead from water using biochars prepared
28
29 from hydrothermal liquefaction of biomass. J. Hazard. Mater. 167, 933–939.
30
31 doi:10.1016/j.jhazmat.2009.01.085
32

33
34 Meng, J., Feng, X., Dai, Z., Liu, X., Wu, J., Xu, J., 2014. Adsorption
35
36 characteristics of Cu(II) from aqueous solution onto biochar derived from
37
38 swine manure. Environ. Sci. Pollut. Res. Int. 21, 7035–46.
39
40 doi:10.1007/s11356-014-2627-z
41

42
43
44 Mohan, D., Kumar, H., Sarswat, A., Alexandre-Franco, M., Pittman, C.U., 2014.
45
46 Cadmium and lead remediation using magnetic oak wood and oak bark fast
47
48 pyrolysis bio-chars. Chem. Eng. J. 236, 513–528.
49
50 doi:10.1016/j.cej.2013.09.057
51

- 1 Ronsse, F., van Hecke, S., Dickinson, D., Prins, W., 2013. Production and
2
3 characterization of slow pyrolysis biochar: influence of feedstock type and
4
5 pyrolysis conditions. *GCB Bioenergy* 5, 104–115. doi:10.1111/gcbb.12018
6
7
8 Shen, Z., Som, A.M., Al-Tabbaa, A., Wang, F., Jin, F., 2015. Three-year impact
9
10 of biochar on the revegetation and mobility of nickel and zinc in an
11
12 industrial contaminated site soil. *Science of The Total Environment*. Under
13
14 review
15
16
17
18 Sohi, S.P., 2012. Agriculture. Carbon storage with benefits. *Science* 338, 1034–
19
20 5. doi:10.1126/science.1225987
21
22
23 Thurkettle, V., 1997. The marketing of British hardwoods. *Forestry* 70, 319–326.
24
25 doi:10.1093/forestry/70.4.319
26
27
28 Yang, Y., Wei, Z., Zhang, X., Chen, X., Yue, D., Yin, Q., Xiao, L., Yang, L., 2014.
29
30 Biochar from *Alternanthera philoxeroides* could remove Pb(II) efficiently.
31
32 *Bioresour. Technol.* 171, 227–232. doi:10.1016/j.biortech.2014.08.015
33
34
35
36
37
38
39
40
41
42
43
44
45
46
47
48
49
50
51
52
53
54
55
56
57
58
59
60
61
62
63
64
65

1 Fig. 1. The Influence of contact time on Pb^{2+} adsorption onto biochar and the fit
2 of the data by Pseudo first order and Pseudo second order models (0.1 g
3 biochar in 20 mL solution (0.01 M $NaNO_3$), initial Pb^{2+} concentration 1mM;
4
5
6 biochar in 20 mL solution (0.01 M $NaNO_3$), initial Pb^{2+} concentration 1mM;
7
8 reaction temperature 20 °C; initial solution pH 5).
9



1 Fig. 2. The influence of biochar dosage (a) and solution pH (b) on the
 2 percentage of lead removal (initial Pb^{2+} concentration 1mM in 20 mL solution
 3 (containing 0.01 M $NaNO_3$), reaction temperature 20 °C, initial solution pH 5,
 4 contact time 24 h), (a) also presents the influence of biochar dosage on the
 5 amount adsorbed per unit of adsorbent mass at equilibrium and (b) also
 6 presents the equilibrium solution pH.

